Finding the Simplest Mechanistic Kinetic Model Describing the Homogeneous Catalytic Hydrogenation of Avermectin to Ivermectin

Mariano D. Cristaldi,[†] María I. Cabrera,[†] Ernesto C. Martínez,[‡] and Ricardo J. A. Grau[†,*]

[†]Instituto de Desarrollo Tecnológico para la Industria Química (INTEC), Universidad Nacional del Litoral (U.N.L.), Consejo Nacional de Investigaciones Científicas y Técnicas (CONICET), CCT-CONICET Santa Fe, Ruta Nacional 168, Km 1, 3000 Santa Fe, Argentina

[‡]Instituto de Desarrollo y Diseño (INGAR), Universidad Tecnológica Nacional (UTN), Consejo Nacional de Investigaciones Científicas y Técnicas (CONICET), Avellaneda 3657, 3000 Santa Fe, Argentina

ABSTRACT: Six mechanistic kinetic models of increasing complexity are analyzed to describe the $RhCl(Ph_3P)_3$ catalyzed hydrogenation process to produce ivermectin from avermectins B_{1a} and B_{1b}. Global sensitivity analysis (GSA) usefulness for selecting the simplest and the most suitable model is shown. First-order and total effect sensitivity indices for model parameters computed from GSA have been used for establishing those elementary reaction steps which were the most important in an extensive reaction framework. The prediction capability of the chosen model is corroborated by comparing its predictions with experimental data from both a lab-scale reactor and an industrial-scale reactor operating under isothermal and nonisothermal conditions, respectively. The best model is simple to use while resulting in a significant computational effort saving because there is no need to perform iterative algorithms for solving model equations. Another interesting feature is that ODEs for such a model have an analytical solution for isothermal hydrogenation processes. These features make modeling more amenable for cost-effective simulation and to include the selected model into computational frameworks for design of the hydrogenation process and control systems of the most usual catalytic method for producing ivermectin.

1. INTRODUCTION

The production of ivermectin (**Iv**) is a leading case of regio-specific homogeneous catalysis found in the fine-chemical industry. Commercial **Iv** is a mixture containing more than 80% ivermectin B_{1a} (**Iv**$_a$) and less than 20% ivermectin B_{1b} (**Iv**$_b$), which is widely used in veterinary medicine against ecto- and endoparasites, including fleas, ticks, lice, mites, flies, and nematodes. Currently, it is also the drug of choice for human onchocerciasis.[1] The synthesis of **Iv** requires the regiospecific hydrogenation of the *cis* carbon—carbon double bond at the 22(23) position of homologous avermectins B_{1a} (**Av**$_a$) and B_{1b} (**Av**$_b$), without affecting the other four carbon—carbon double bonds at the 3(4), 8(9), 10(11), and 14(15) positions of the cyclic lactone moiety (see Scheme 1). In current practice, the hydrogenation process is catalyzed by Rh or Ir precursors modified with tertiary phosphines, typically triphenylphosphine in homogeneous systems,[2,3] and sulphonated aryl phosphines in biphasic systems.[4−6] The most usual catalyst is chlorotris(triphenylphosphine)rhodium(I) (Wilkinson's catalyst).

Since **Iv** became a generic drug in the middle 1990s, an increasing competence has depressed its price for years, while the Rh price continued to climb. In this scenario, batch process design and optimization for operational profitability improvement has gained increasing importance because the industrial productions to be withdrawn from the market will be the costliest.

Most of the information on the **Iv** synthesis processes has been reported in patents of invention, which are somewhat circumspect in revealing kinetic details, and is much less model related. Moreover, compared with other reaction systems, only a few kinetic models are so far available from the open literature.[7,8]

Complex reaction networks could be invoked to describe this reacting system; however, very refined descriptions would involve too many adjustable parameters for performing unambiguous estimates within a framework of overall kinetic measurements. In fact, the associated reaction network describing the full catalytic cycle with Wilkinson's catalyst $[RhCl(Ph_3P)_3]$ is shown in Scheme 2. This network admits up to 18 adjustable kinetic parameters, and kinetic models involve differential-algebraic nonlinear systems, which have to be numerically solved by iterative procedures. Thus, the structure of the best-fitting model could be quite complex and particularly impractical when applied to kinetic modeling for the analysis and design of the chemical process and its control system. Indeed, most of the engineers working in these fields have a conspicuous preference for adopting mathematical models as simple as possible to describe the reaction process. In this prevailing scenario, the modeling purpose is not to build extremely complex models to fully explain the underlying reaction mechanism, instead the target is to construct the simplest model capable of providing a reliable prediction of the kinetic behavior. From this viewpoint, we propose that a special challenge is basically not about what to include in the kinetic model, but instead what can be overlooked (if possible). Thus, to have as few adjustable parameters as possible, our current task is to find the simplest plausible, encompassing kinetic model able to explain the overall significant effects with a suitable predictive capability when an industrial

Scheme 1. Regio-specific Hydrogenation of Avermectin B$_1$ (Series *a* and *b*) for Producing Ivermectin
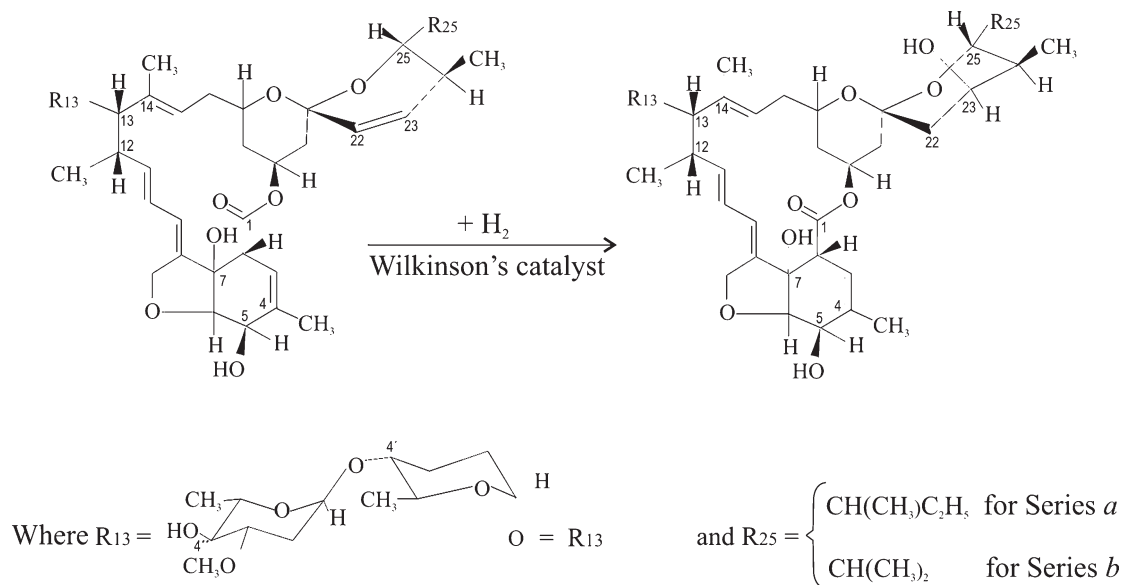
Scheme 2. Reaction Network for the RhCl(PPh$_3$)$_3$ Catalyzed Hydrogenation of Avermectins[7,8]
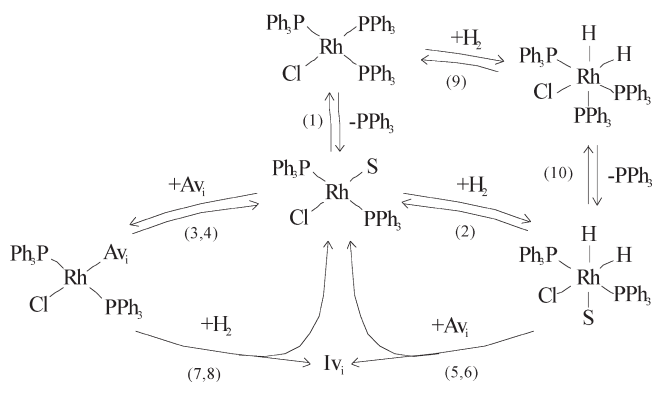
operating window for handle variables has been defined. The formulation of the simplest kinetic model thus involves some sort of reaction pathways. In such an approach, the focus is on determining the most important reaction pathways to reduce model complexity until the simplest kinetic model is found.

Sensitivity analysis (SA) is a tool easy to use and integrate with the classical procedure of minimizing the sum of square residuals and judging if a rival model should be rejected or accepted on the basis of statistical criteria. More specifically, the variance-based global SA (GSA) is a reliable method for quantifying the relative importance of all parameters and their interactions on the model output when parameter values are changed simultaneously into the parametric uncertainty domain.[9−15] Thus, model parameters can be ranked in order from the most influential to the less influential ones. This arrangement provides both qualitative and quantitative insight into which meaningful subset of parameters needs to be accurately determined and those less relevant parameters that could be kept constant in their variation intervals or excluded for model simplification purposes without a loss in model predictions.[16] GSA has been used in the analysis of complex models including identification of calibration variables, model simplification,

and model quality assurance.[17,18] Despite many advantages of GSA, its application in chemical reaction engineering is still scarce.

This contribution aims at presenting the main features which have resulted after integrating GSA into our research activities for selecting the simplest kinetic model to describe the most usual catalytic hydrogenation process to obtain **Iv** from **Av**. Kinetic modeling is performed on the basis of mechanistic knowledge of underlying catalytic processes and using experimental kinetic data from a lab-scale reactor. Experimentation is planned to cover the operational space defined constraints in an industrial process. Six possible candidate kinetic models accounting for different reaction pathways are examined. The usefulness of GSA for selecting the simplest and suitable model from the set of possible candidates is shown. Finally, the prediction capability of the chosen model is corroborated by comparing its predictions with experimental data from an industrial-scale reactor operating under nonisothermal conditions.

2. KINETIC MODEL FORMULATION

2.1. Reaction Mechanism and Kinetic Models. Different reaction pathways of increasing complexity are examined within the reaction network previously suggested from our laboratory.[7,8] Six possible kinetic models, herein below referred to as M1, M2, ..., and M6, are scrutinized. The underlying reaction arises from different combinations of elementary reaction steps as summarized in Table 1. Further peripheral elementary reaction steps are known to be auxiliary and, therefore, not included to avoid overparameterized models. Scheme 2 is drawn for easier viewing of mechanistic differences between models.

Main simplifying assumptions in deriving overall reaction rates and species balance equations are (1) the reversible reactions are at equilibrium; (2) the hydrogen transfer to 22(23) carbon−carbon double bond is a rate-determining step (RDS); (3) there is no deactivation of catalytic species in reacting solution; (4) the formation of multihydrogenated species is negligible due to low reaction temperature; (5) the gas−liquid hydrogen-transfer is not RDS; and, (6) perfect mixing.

4253

dx.doi.org/10.1021/ie101289h |*Ind. Eng. Chem. Res.* 2011, 50, 4252–4263

Table 1. Elementary Reaction Steps of Avermectin Hydrogenation with Wilkinson's Catalyst[a].

elementary steps	parameters	basic routes					
		M1	M2	M3	M4	M5	M6
(1) $RhCl(Ph_3P)_3 + S \rightleftharpoons RhCl(Ph_3P)_2S + Ph_3P$	$K_0, -\Delta H_0$	0	0	1	1	1	1
(2) $RhCl(Ph_3P)_2S + H_2 \rightleftharpoons RhCl(Ph_3P)_2(H)_2S$	$K_1, -\Delta H_1$	1	1	1	1	1	1
(3) $RhCl(Ph_3P)_2S + Av_a \rightleftharpoons RhCl(Ph_3P)_2Av_aS$	$K_{2a}, -\Delta H_{2a}$	1	1	0	1	1	1
(4) $RhCl(Ph_3P)_2S + Av_b \rightleftharpoons RhCl(Ph_3P)_2Av_bS$	$K_{2b}, -\Delta H_{2b}$	1	1	0	1	1	1
(5) $RhCl(Ph_3P)_2(H)_2S + Av_a \rightarrow RhCl(Ph_3P)_2S + Iv_a$	k_{3a}, E_{3a}	1	1	1	1	1	1
(6) $RhCl(Ph_3P)_2(H)_2S + Av_b \rightarrow RhCl(Ph_3P)_2S + Iv_b$	k_{3b}, E_{3b}	1	1	1	1	1	1
(7) $RhCl(Ph_3P)_2Av_aS + H_2 \rightarrow RhCl(Ph_3P)_2S + Iv_a$	k_{4a}, E_{4a}	0	1	0	0	1	1
(8) $RhCl(Ph_3P)_2Av_bS + H_2 \rightarrow RhCl(Ph_3P)_2S + Iv_b$	k_{4b}, E_{4b}	0	1	0	0	1	1
(9) $RhCl(Ph_3P)_3 + H_2 \rightleftharpoons RhCl(Ph_3P)_3(H)_2$	$K_5, -\Delta H_5$	0	0	0	0	0	1
(10) $RhCl(Ph_3P)_3(H)_2 + S \rightleftharpoons RhCl(Ph_3P)_2(H)_2S + Ph_3P$	$K_6, -\Delta H_6$	0	0	0	0	0	1
number of independent parameters		10	14	8	12	16	18

[a] "Av" and "Iv" denote avermectin and ivermectin, respectively; "a" and "b" subscripts represent series A and B, respectively.

Under these assumptions, the hydrogenation rate of **Av** to **Iv**, with distinction of series a and b, can be mathematically described by the following differential-algebraic equation systems

$$\frac{d[Av_i]}{dt} = -k_{3i}K_1(1 + \Theta\hat{k}_{4i}\hat{K}_{2i})[H_2][RhCl(Ph_3P)_2S][Av_i],$$

$$i = a, b \qquad (1)$$

$$[Av_i] = [Av_i]_0, \quad t = 0 \qquad (2)$$

$$[Iv_i] = [Av_i]_0 - [Av_i], \quad t > 0 \qquad (3)$$

where

$$\Theta = \begin{cases} 0, & \text{for M1, M3, and M4} \\ 1, & \text{for M2, M5, and M6} \end{cases} \qquad (4)$$

$$\hat{k}_{4i} = \frac{k_{4i}}{k_{3i}} \qquad (5)$$

$$\hat{K}_{2i} = \frac{K_{2i}}{K_1} \qquad (6)$$

and with the additional relationship resulting from the principle of microscopic reversibility

$$K_0K_1 = K_5K_6, \quad \text{for M6} \qquad (7)$$

In eqs 1, the concentration of the catalytic species $RhCl(Ph_3P)_2S$ is governed by the following relationships arising from the balances on species having Rh and Ph_3P:

$$[RhCl(Ph_3P)_2S] - \frac{[Rh]_0}{1 + K_1[H_2] + K_{2a}[Av_a] + K_{2b}[Av_b]}$$

$$= 0, \quad \text{for M1 and M2} \qquad (8)$$

$$[RhCl(Ph_3P)_2S]^2 + K_0[RhCl(Ph_3P)_2S] - \frac{K_0[Rh]_0}{1 + K_1[H_2]}$$

$$= 0, \quad \text{for M3} \qquad (9)$$

$$[RhCl(Ph_3P)_2S]\left\{1 + \frac{1}{K_0}[RhCl(Ph_3P)_2S]\right\}$$

$$- \frac{[Rh]_0}{1 + K_1[H_2] + K_{2a}[Av_a] + K_{2b}[Av_b]} = 0, \quad \text{for M4 and M5} \qquad (10)$$

$$[RhCl(Ph_3P)_2S]\left\{1 + \frac{(1 + K_5[H_2])}{K_0}[RhCl(Ph_3P)_2S]\right\}$$

$$- \frac{[Rh]_0}{1 + K_1[H_2] + K_{2a}[Av_a] + K_{2b}[Av_b]} = 0, \quad \text{for M6} \qquad (11)$$

Notice that estimates of $[RhCl(Ph_3P)_2S]$ have to be performed by an iterative process at each reaction time, except for model M3, which provides an explicit mathematical expression for the concentration of this catalytic species for both isothermal and isobaric systems.

To complete the model formulation, the functional dependence of the equilibrium and kinetic parameters with temperature is described by the van't Hoff equation

$$K_i(T) = K_i(T_r)\exp\left(-\frac{\Delta H_i}{RT'}\right) \qquad (12)$$

and the Arrhenius equation

$$k_i(T) = k_i(T_r)\exp\left(-\frac{E_i}{RT'}\right) \qquad (13)$$

respectively, where T' is defined as

$$\frac{1}{T'} = \frac{1}{T} - \frac{1}{T_r} \qquad (14)$$

and T_r is the chosen reference temperature.

2.2. General Approach for Solving the Kinetic Models. The differential-algebraic equation systems to be solved can concisely be written as follows

$$\frac{d}{dt}\mathbf{y}^k(t) = f(\mathbf{y}^k(t), \mathbf{z}^k(t), \boldsymbol{\theta}^k, \mathbf{w}^k), \quad 0 < t \leq \Gamma,$$

$$\mathbf{y}^k(0) : \text{given} \tag{15}$$

$$\mathbf{z}^k(t) = f(\mathbf{y}^k(t), \boldsymbol{\theta}^k, \mathbf{w}^k) \tag{16}$$

where k stands for the models, $\mathbf{y}^k(t)$ is an n-dimensional vector of predicted concentrations of bulk species, $\mathbf{z}^k(t)$ is an m-dimensional vector of concentrations of the active catalytic species, $\boldsymbol{\theta}^k$ is a p^k-dimensional vector of kinetic parameters, $\mathbf{w}^k$ is a q^k-dimensional vector of known parameters representing operational conditions, and Γ is the batch-completion time.

Accepting that only the dependent variables $\mathbf{y}^k(t)$ are subject to error, $\boldsymbol{\theta}^k$ is optimized by minimizing the residual sum of squares (RSS)

$$\text{RSS}^k = \min_{\boldsymbol{\theta}^k \in \Theta^k} \{tr[(\mathbf{Y}^k(\boldsymbol{\theta}^k) - \mathbf{Y}^{\text{exp}})^T(\mathbf{Y}^k(\boldsymbol{\theta}^k) - \mathbf{Y}^{\text{exp}})]\} \tag{17}$$

where $\mathbf{Y}^k(\boldsymbol{\theta}^k)$ and $\mathbf{Y}^{\text{exp}}$ are matrices arranging the sets of concentration−time predictions $\mathbf{y}^k$ and experimental data $\mathbf{y}^{\text{exp}}$, respectively, and Θ^k is the allowable parametric domain.

In the classical approach all the elements (parameters) of $\boldsymbol{\theta}^k$ are optimized without distinction until the minimum of RSS^k is achieved. Distinctively, GSA can be used to identify which subset of $\boldsymbol{\theta}^*$ accounts for most of RSS^k variance and in what extent it can be explained by uncertainty sources. Thus, for improving estimation accuracy and reducing complexity, the parameters identified as less sensitive can be fixed to any value within the upper and lower values of their confidence bounds[19] and so only the most influencing ones have to be optimized. To take advantage of this feature, we have included GSA in our model-building strategy.

Model selection was performed using AIC (Akaike Information Criterion),[20] which is by definition

$$\text{AIC}^k = 2p + N \ln(\text{RSS}^k) \tag{18}$$

where N is the total experimental data used for parameters estimation. From AIC point of view, the more adequate kinetic model is which has the lowest value for the AIC index.

Our approach consists of four steps: (1) rough parameter estimation; (2) sensitive parameter estimation; (3) predictive capability evaluation; and, (4) extended performance evaluation. All candidate models are intentionally kept until a more comprehensive analysis is made on the basis of new information from experimental runs at the laboratory-scale and industrial-scale. To cover the operational window of the process with the smallest possible number of experiments, central composite design (CCD) is chosen to perform the laboratory-scale experiments selecting temperature and catalyst loading as independent variables. Data sets from axial points are used as the basis for rough parameter estimation (Step 1). Data set from the central point is used to identify the most sensitive parameters and further to re-estimate such parameters while keeping unchanged the values of the less influential ones as "true" (Step 2). New data for model updating are thus used in a more informative way. This procedure will have some influence on the fitted parameters if the correlation structure is significant, but it is adopted because the dimensionality of the parameter subset of $\boldsymbol{\theta}^k$ being optimized could be reduced to a few parameters. After most relevant

parameters have been reestimated, the interpolation capability is tested for all the models by evaluating prediction accuracy using new data collected within the experimental domain bounded by the axial points (step 3). The simplest possible kinetic model comes from a balance between data fitting capability and model complexity. Model performance assessment is finally performed by comparing theoretical predictions with experimental data from an industrial-scale reactor (step 4).

2.3. GSA and Sensitivity Indices Computation. To ascertain the parameter subset of $\boldsymbol{\theta}^k$ that account for most of the J^k variance, either by themselves or due to overall interactions with other parameters, the first-order sensitivity (S_i^k) and total effect sensitivity (ST_i^k) indices are calculated as follows

$$S_i^k = \frac{V(\theta_i^k)}{V(Y^k)} \tag{19}$$

$$\text{ST}_i^k = 1 - \frac{V(\theta_{-i}^k)}{V(Y^k)} \tag{20}$$

where $V(\theta_i^k)$ is the conditional variance of the parameter θ_i^k of the set of p^k parameters interacting among them, $V(\theta_{-i}^k)$ is the contribution to the variance of the Y^k output response attributable to the $p^k - 1$ remaining parameters, and $V(Y^k)$ is the unconditional variance of Y^k which, in turn, is composed as follows:

$$V(Y^k) = \sum_i V(\theta_i^k) + \sum_i \sum_{j>i} V(\theta_i^k, \theta_j^k) + \dots + V(\theta_1^k, \theta_2^k, \dots, \theta_p^k) \tag{21}$$

where $V(\theta_i^k, \theta_j^k)$ is the variance of the interaction between parameters θ_i^k and θ_j^k, and so on until the parameter set is complete.

Estimators for S_i^k and ST_i^k are based on a variety of approaches.[15,21−23] An improved Sobol's method was chosen to generate a quasi-random sampling in the multidimensional space spanned by Θ^k.[24] Parameter uncertainties were assumed to be independent, and feasible values of parameters were described by uniform distributions bounded by the lowest and highest values in the interval defined by a percentage of default values. Uniform distributions were assumed due to the lack of knowledge about the true distributions. Representative samples of model parameter values were generated using the Marsaglia's Subtract-with-Borrow algorithm, implemented in the MATLAB language. This algorithm is a pseudorandom number generator which theoretically can generate over 2^{1492} double precision values before repeating itself.[25] A preliminary study of the convergence of the sensitivity indices allowed us to set 1000 Monte Carlo simulations per parameter, which leads to 8000−18000 parameter combinations depending on the kinetic model.

2.4. Parameter Confidence Limits Computation. Nonlinear regression parameters confidence intervals were computed as follows: (1) the minimum value of the objective function ($\text{RSS}_{\text{min}}^k$) was obtained from the set of RSS^k values generated by Monte Carlo simulations; (2) the maximum value of the objective function ($\text{RSS}_{\text{max}}^k$) was defined for a given value of confidence (α); (3) the set of parameter values $\boldsymbol{\theta}^k$ was picked out if $\text{RSS}^k \in [\text{RSS}_{\text{min}}^k; \text{RSS}_{\text{max}}^k]$, otherwise it was excluded; and (4) the confidence limits of each parameter were calculated for $(1 - \alpha)\%$ confidence level once a representative set of $\boldsymbol{\theta}^k$ was acquired after a sufficiently great number of simulations were made. The parameter α was settled equal to 0.05.

Table 2. Experimental Conditions for Parameter Estimation and Model Selection

experimental run	temperature (K)	catalyst loading[a] (% mol RhCl(Ph$_3$P)$_3$/mol Av)
1[b]	298	1.06
2[b]	298	7.26
3[b]	328	1.06
4[b]	328	7.26
5[c]	313	3.55
6[d]	298	2.05
7[d]	313	2.05
8[d]	328	2.05
9[d]	313	7.26

[a] Initial ratio. [b] Data for rough estimation of parameters. [c] Data for optimization of the most relevant parameters. [d] Data for testing the interpolation capability of models.

3. EXPERIMENTAL SECTION

3.1. Experimental Strategy. The experimental conditions of the Composed Central Design are summarized in Table 2. The axial points were chosen so as to widely cover the operation window of industrial hydrogenation processes. The experimental domain was stated taking into account the following features: (i) the hydrogenation rate is very slow at temperatures lower than 298 K, requiring therefore excessively long reaction times; (ii) a selectivity loss yielding undesirable tetra-hydrogenated derivatives takes place at temperatures higher than 328 K; (iii) catalyst loadings lower than 0.50% demand quite long reaction times and non-negligible deactivation of catalytic species; whereas catalyst loadings higher than 7% are excessively high because the gas-to-liquid hydrogen mass transfer effects are not negligible and, mainly, at this loading the catalytic process becomes uneconomical.

The rough parameter estimation was carried out by fitting model predictions to **Av** and **Iv** (series a and b) concentrations versus time data at the axial points (184 experimental data). An initial estimation of all kinetic parameters (K_i and k_i) was performed using experimental data obtained at the reference temperature of 298 K and covering the catalyst loading and time (conversion) domains of interest (runs 1 and 2, 88 experimental data). Afterward, a first estimation of enthalpy changes ($-\Delta H_i$) and activation energies (E_i) was done using experimental data covering the temperature and time (conversion) domains (runs 3 and 4, 96 experimental data). The temperature parametrization was according to eqs 12−14. The resulting rough estimates were assigned as default values (not shown) to perform GSA. S_i^k and ST_i^k were computed to identify the subset of model parameters that contribute the most to the variance of RSS^k at the central point (run 5, 48 experimental data). Assessment of the interpolation capability of models considered was made using new data sets within the experimental domain of interest (experimental runs 6−9, 204 experimental data). Appraisal of application performance of the simplest kinetic model was made using experimental data from an industrial-scale reactor (run 10, 12 experimental data).

3.2. Experimental Procedures. Laboratory-scale experimental data are from a previous study at this laboratory, which was carried out in a 300 mL laboratory-scale reactor operated under isothermal semibatch mode. Experimental laboratory setup and procedures ensured complete induction time suppression, negligible gas-to-liquid resistance for hydrogen mass-transfer, the absence of catalytic complexes deactivation, and good data reproducibility. Complete details can be found in a previous contribution.[7]

Industrial-scale experimental data from a 50 L mechanically stirred industrial reactor operated under nonisothermal semibatch mode are used to evaluate the application performance of the simplest kinetic model that provides a satisfactory description of laboratory data. A typical industrial-scale hydrogenation run was as follows: A toluene solution of purified avermectin (50 L, 13.87 wt %) and a precise amount of catalyst (28 g, 0.50 wt %) were charged into the reactor vessel at room temperature. The reactor was assembled, degassed by mild vacuum, purged three times, and flushed with hydrogen at room temperature. After complete dissolution of the catalyst, the reactor was pressurized with hydrogen gas and, while reacting, heated up to the settled reaction temperature. The hydrogenation was allowed to continue until at least 98% of **Av** conversion.

3.3. Analytical Method. Samples of the reaction mixture were withdrawn from the industrial-scale reactor at different time intervals for determination of **Av** and **Iv** concentrations (with resolution of series a and b) by HPLC. The analyses were performed on a liquid chromatograph (Shimadzu LTO-10A/LC-10AS) equipped with a diode-array detector (Shimadzu SPD-M10A), using a C18 column (Nucleosil C18, 150 mm × 4.6 mm ID, 5 μm) under the following conditions: acetonitrile/methanol/water (28:56:16) as mobile phase; flow rate, 1 mL/min; detection, UV, 246 nm; temperature, 303 K.

3.4. Effects of the Gas-to-Liquid Hydrogen Mass-Transfer. Modeling was made under the following underlying assumptions: (a) The hydrogen transfer rate is proportional to the area of the gas bubbles and to the concentration gradient at the gas−liquid interface. (b) On the gas-phase side, there exists no appreciable mass transfer resistance because the gas phase contains practically pure hydrogen and the diffusion phenomenon in the gas phase is about 2 orders of magnitude faster than in the liquid phase. (c) The overall resistance is therefore only due to the hydrogen diffusion through the liquid films around the gas bubbles. (d) The bubbles are homogeneously dispersed into the liquid phase when operating the 4-baffled mechanically agitated reactor, with a six-bladed turbine stirred, at 1750 rpm. (e) The hydrogen solubility in the toluene liquid phase is practically not affected by the presence of solubilized macrocyclic lactones. (f) There is no accumulation of hydrogen in the bulk liquid phase; that is, all the hydrogen tranferred through the gas−liquid interface is just consumed by chemical reaction. (g) The overall mass transfer parameter at the gas−liquid interface can be acceptably estimated from empirical correlations expressed in terms of physicochemical properties of the system and the stirring rate or the power input.

Values of the hydrogen concentration drop at the gas−liquid interface were calculated from theoretical estimates of the gas−liquid overall mass-transfer coefficient ($k_b a_b$) and measured hydrogen consumption rates (r_H^{exp}). From a correlation expressed in terms of the physical properties of the reaction mixture and operating conditions,[26] the minimum value of $k_b a_b$ was found to be about 5.00×10^{-1} s^{-1}. The maximum value of r_H^{exp} was about 2.5×10^{-5} mol L^{-1} s^{-1}. The concentration of dissolved hydrogen was estimated using data of hydrogen solubility in benzene.[27] The value of the relative drop of the hydrogen concentration at the gas−liquid interface was consequently

4256

dx.doi.org/10.1021/ie101289h |*Ind. Eng. Chem. Res.* 2011, 50, 4252–4263

Table 3. Estimated Values of Sobol's First-Order and Total Sensitivity Indices for the Six Kinetic Models

parameter i	M1 S_i^1	ST_i^1	M2 S_i^2	ST_i^2	M3 S_i^3	ST_i^3	M4 S_i^4	ST_i^4	M5 S_i^5	ST_i^5	M6 S_i^6	ST_i^6
K_0					0.03	0.15	0.02	0.14	0.02	0.16	0.01	0.12
K_1	0.03	0.27	0.03	0.32	0.03	0.29	0.05	0.30	0.05	0.30	0.04	0.25
K_{2a}	0.00	0.00	0.00	0.00			0.00	0.00	0.00	0.00	0.00	0.00
K_{2b}	0.00	0.00	0.00	0.00			0.00	0.00	0.00	0.00	0.00	0.00
K_5											0.02	0.11
k_{3a}	0.14	0.59	0.08	0.57	0.08	0.08	0.11	0.48	0.09	0.49	0.09	0.44
k_{3b}	0.00	0.00	0.00	0.00	0.00	0.00	0.00	0.00	0.00	0.00	0.00	0.00
k_{4a}			0.00	0.00					0.00	0.00	0.00	0.00
k_{4b}			0.00	0.00					0.00	0.00	0.00	0.00
$-\Delta H_0$					0.01	0.15	0.00	0.02	0.01	0.12	0.02	0.10
$-\Delta H_1$	0.02	0.25	0.03	0.30	0.02	0.27	0.02	0.24	0.04	0.25	0.03	0.23
$-\Delta H_{2a}$	0.00	0.00	0.00	0.00			0.00	0.00	0.00	0.00	0.00	0.00
$-\Delta H_{2b}$	0.00	0.00	0.00	0.00			0.00	0.00	0.00	0.00	0.00	0.00
$-\Delta H_5$											0.00	0.10
E_{3a}	0.13	0.58	0.12	0.56	0.02	0.27	0.08	0.45	0.05	0.41	0.06	0.38
E_{3b}	0.00	0.00	0.00	0.00	0.06	0.46	0.00	0.00	0.00	0.00	0.00	0.00
E_{4a}			0.00	0.00					0.00	0.00	0.00	0.00
E_{4b}			0.00	0.00					0.00	0.00	0.00	0.00

lower than 2%. This estimation is expected to be conservative because the amphiphatic bisoleandrosyloxy group attached to position C-13 of the avermectin macromolecule confers to this macrocyclic lactone surface activity that promotes interfacial area generation. Thus, under the experimental conditions used in the industrial-scale hydrogenation run, the hydrogen mass transfer effects on the reaction rate were found to be practically negligible.

4. RESULTS AND DISCUSSION

Implementation of the GSA gave the results summarized in Table 3. Results show that there are only a few parameters, strongly interacting, that have a significant influence on the variance of RSS^k, and it could determine the main mechanism for sensitivity. Analysis based on values of S_i^k and ST_i^k indices may allow an ordering of the elementary reaction steps that reveals the high significance of the "hydride route" (steps 2, 5, and 6) with respect to the "olefin route" (steps 3, 4, 7, and 8), whichever the model. In fact, parameters K_1, $-\Delta H_1$, k_{3a}, and E_{3a} explain most of the variance of RSS^k and their individual ST_i^k values reveal a strong interaction. Parameters K_{2a}, $-\Delta H_2$, k_{4a}, and E_{4a} have hardly, if not null, significative effects. The parameters associated to the b homologous species also have null effects due to the relatively lower content of species series b in the reaction mixture. The conclusion of a prevailing reaction pathway through the "hydride route" is also drawn after including the simple dissociation of the catalyst precursor (step 1). Indeed, the variance of RSS^k is slightly sensitive to the individual effects of K_0 and $-\Delta H_0$, but the parameter values are strongly related to those of K_1, $-\Delta H_1$, k_{3a}, and E_{3a}. The inclusion of peripheral pathways, such as the pathway involving the dihydride complex RhCl-$(Ph_3P)_3(H)_2$ (steps 9 and 10), introduce additional uncertainty sources that have little individual influence on the variance of RSS^k, which is in turn spread over a major number of parameters due to strong interaction effects.

Table 4. Estimated Values of RSS and AIC for the Six Kinetic Models at Experimental Conditions for Parameter Estimation

experimental run	$RSS \times 10^4$ [mol^2 L^{-2}] M1	M2	M3	M4	M5	M6
1	3.37	2.26	0.076	0.148	0.119	0.154
2	4.70	5.37	0.876	0.498	0.565	0.473
3	6.51	7.63	0.114	0.046	0.136	0.043
4	1.25	0.68	0.128	0.269	0.292	0.257
5	0.19	0.17	0.044	0.022	0.016	0.015
AIC	−1190	−1181	−1675	−1711	−1677	−1707

Notice that sensitive parameters can individually explain a moderate percentage of the RSS^k variance but its importance in model parametrization is due to a significant parameter interaction in the model structure. Moreover, it is worth noting that the recognizable pattern of sensitivity can be linked to pioneering findings in hydrogenation processes of shorter olefins catalyzed with tris(triphenylphosphine)halogeno−rhodium(I) complexes. Certainly, it can be stated that there is a substantial correspondence between the insights into the main reaction pathway that arise from GSA results and those supported by careful kinetic[28−43] and spectroscopic[44,45] studies.

From the clear pattern of sensitivity, the parameters K_0 and $-\Delta H_0$ (except for models M1 and M2), and K_1, $-\Delta H_1$, k_{3a}, and E_{3a} (for all models) were re-estimated fixing all the other model parameters within their variability intervals. Table 4 summarizes the RSS^k and AIC^k estimated values for each model at conditions of experimental runs 1−5 used for parameters estimation. The RSS^k values at the central point are one-order of magnitude lower than those at the axial conditions, revealing that the main uncertainty sources in the models were identified by GSA. A comparison of AIC^k values reveals that models M1 and M2 provide the worst quality of the kinetic description because the objective function values are 1 order of magnitude greater than those characterizing models M3−M6, which in turn were found to be nearly equally capable of describing the experimental data.

Figure 1 illustrates the predicted and experimental concentrations of **Av** and **Iv** as a function of the hydrogenation time, for models M1−M6. In accordance with AIC^k values, a simple visual inspection reveals that models M1 and M2 are less suitable than models M3−M6, and that the latter models have a similar capability to fit laboratory experimental values. The first-order and half-order dependences of the hydrogenation rate on the catalyst loading is the common difference between both groups of models, as stated by eq 8 and eqs 9−11, respectively. In agreement with our previous findings,[7] this quality indicates that the dissociative pathway for RhCl(PPh$_3$)$_3$ plays a major role and cannot be omitted (step 1). The powerful data fitting capability arising from GSA seems to reinforce this conclusion since it reveals a structural deficiency of models including complete dissociation of RhCl(PPh$_3$)$_3$. Table 5 summarizes the optimized values of parameters for 95% confidence boundary limits. The differences between the estimates of various parameters are apparent, but the values are basically within the typical range of those reported for the hydrogenation of diverse olefins. Consequently, so far there is no base on which to discriminate among models M3−M6.

In a further attempt to discriminate among candidate models M3−M6, their interpolation capability was evaluated in terms of the prediction accuracy of new data sets within the experimental
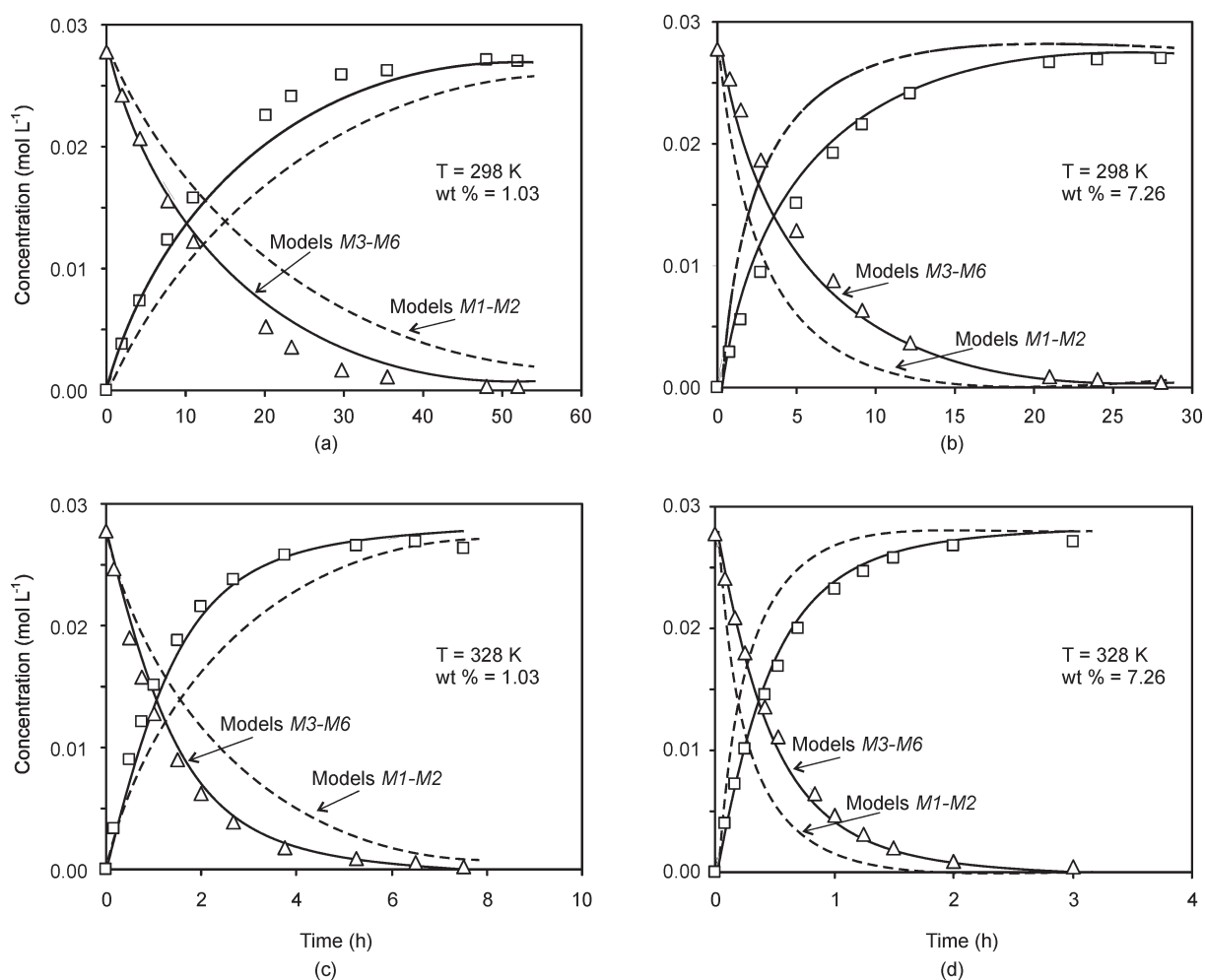
Figure 1. Experimental and predicted profiles during the hydrogenation of avermectin (2.8 mmol) in toluene solution (100 mL), for different Wilkinson's catalyst loadings, at 298 and 313 K, and hydrogen pressure of 275.7 kNm^{-2}. Dotted lines illustrate predictions of models M1 and M2. Full lines illustrate predictions of models M3−M6.

domain of interest (experimental runs 6−9). Table 6 summarizes the RSS^k and AIC^k values obtained in these calculations. The accuracy of models seems to be temperature dependent, the higher the temperature is, the lower is the predictive capability of all models. The lowest AIC value is obtained for the model M3. Data prediction quality is, however, almost the same for these four models despite the number of adjustable parameter increase from 8 (model M3) to 18 (model M6). We therefore have taken the simplest model M3 as a comparison base to address some issues about increasing model complexity:

(1) The addition of short olefins (e.g., cyclohexene) to the catalytic species RhCl(Ph$_3$P)$_2$S has been experimentally inferred by Wilkinson and co-workers.[28] Accordingly, the addition of **Av**$_i$ to RhCl(Ph$_3$P)$_2$S yielding RhCl(Ph$_3$P)$_2$Av$_i$S was included in the full reaction network. GSA distinctly reveals that K_{2a}, $-\Delta H_{2a}$, K_{2b}, and $-\Delta H_{2b}$ are no-sensitive parameters and, consequently, the inclusion of reaction steps 3 and 4 does not significantly improve the fit quality but the number of adjustable parameters increases from 8 (model M3) to 12 (model M4). Our conjecture to explain this behavior is that larger olefins, as these macrocyclic lactones, have less chances than shorter olefins to compete with the small hydrogen molecules for the catalytic species RhCl(Ph$_3$P)$_2$S favoring, still more, the prevailing formation of the hydride complex RhCl(PPh$_3$)$_2$(H)$_2$(S) on the olefin complex RhCl(Ph$_3$P)$_2$Av$_i$S.

(2) The hydrogen transfer to olefin complexes seems to be unlikely to occur due to the low capability of olefin complexes to activate hydrogen.[28] The hydrogen addition to complexes RhCl-(Ph$_3$P)$_2$Av$_i$S, followed by hydrogen transfer to 22(23) carbon−carbon double bond yielding **Iv**$_i$ and restoring RhCl(Ph$_3$P)$_2$S to the catalytic cycle, was however included as lumped steps to analyze the effects of including the overall "olefin route". GSA clearly indicates that k_{4a}, E_{4a}, k_{4b}, and E_{4b} are no-sensitive parameters and confirms that the further inclusion of steps 7 and 8 does not improve the data fitting capability either. This result leads to the conclusion that the catalytic hydrogenation process of these macrocyclic lactones does not significantly involve the basic pathway referred to as "olefin route", as suggested for short olefins. Thus, the complete inclusion of this pathway only increases the number of adjustable parameters from 8 (model M3) to 16 (model M5).

(3) The additional formation of the complex RhCl(PPh$_3$)$_2$-(H)$_2$(S) through the dihydride complex RhCl(PPh$_3$)$_3$(H)$_2$ is invoked in full catalytic cycle of olefin hydrogenation by Wilkinson's catalyst. We have previously concluded in favor of including steps 9 and 10 because when omitting this peripheral pathway in the reaction mechanism the resulting value of K_0 is not comparable to that measured in pure benzene.[8,46] In fact, the main difference between models M3−M5 is around the

Table 5. Estimated Kinetic Model Parameters for 95% Confidence Limits

parameter	M1	M2	M3	M4	M5	M6
				kinetic model		
K_0 (M) [a]			$(1.59 \pm 0.39) \times 10^{-7}$	$(5.42 \pm 0.09) \times 10^{-7}$	$(1.06 \pm 0.02) \times 10^{-6}$	$(8.19 \pm 0.11) \times 10^{-5}$
K_1 (M^{-1}) [a]	$(7.39 \pm 0.13) \times 10^1$	$(4.74 \pm 0.07) \times 10^1$	$(1.90 \pm 0.04) \times 10^2$	$(1.76 \pm 0.03) \times 10^2$	$(1.65 \pm 0.02) \times 10^2$	$(1.61 \pm 0.02) \times 10^1$
K_{2a} (M^{-1})	$(3.70 \pm 0.07) \times 10^{-1}$	$(7.21 \pm 0.11) \times 10^{-3}$		$(5.78 \pm 0.10)10^{-1}$	$(3.08 \pm 0.05) \times 10^{-1}$	$(3.08 \pm 0.04) \times 10^{-1}$
K_{2b} (M^{-1})	$(3.29 \pm 0.07) \times 10^{-1}$	$(6.97 \pm 0.11) \times 10^{-3}$		$(5.77 \pm 0.09)10^{-1}$	$(2.93 \pm 0.04)10^{-1}$	$(2.79 \pm 0.04) \times 10^{-1}$
K_5 (M^{-1}) [a]						$(8.02 \pm 0.11) \times 10^1$
k_{3a} (M s)$^{-1a}$	$(1.38 \pm 0.02) \times 10^{-1}$	$(2.05 \pm 0.03) \times 10^{-1}$	3.87 ± 0.07	2.11 ± 0.03	1.62 ± 0.02	1.36 ± 0.02
k_{3b} (M s)$^{-1}$	$(9.00 \pm 0.02) \times 10^{-2}$	$(1.67. \pm 0.02) \times 10^{-1}$	3.60 ± 0.07	1.90 ± 0.03	1.45 ± 0.02	1.16 ± 0.01
k_{4a} (M s)$^{-1}$		$(6.03 \pm 0.09) \times 10^{-4}$			$(4.96 \pm 0.07) \times 10^{-3}$	$(2.14 \pm 0.03) \times 10^{-4}$
k_{4b} (M s)$^{-1}$		$(4.86 \pm 0.08) \times 10^{-3}$			$(6.10 \pm 0.09) \times 10^{-5}$	$(1.00 \pm 0.01) \times 10^{-4}$
$-\Delta H_0$ (kJ mol^{-1}) [a]			9.20 ± 1.20	4.10 ± 0.96	0.40 ± 0.82	2.20 ± 0.73
$-\Delta H_1$ (kJ mol^{-1}) [a]	-0.60 ± 0.90	-8.90 ± 0.86	-0.60 ± 1.10	0.00 ± 0.80	-0.70 ± 0.85	1.30 ± 0.71
$-\Delta H_{2a}$ (kJ mol^{-1})	1.50 ± 0.92	1.50 ± 0.81		1.60 ± 0.92	2.10 ± 0.85	$(2.63 \pm 0.07) \times 10^1$
$-\Delta H_{2b}$ (kJ mol^{-1})	2.00 ± 1.00	2.20 ± 0.83		2.40 ± 0.95	2.00 ± 0.83	$(2.49 \pm 0.07) \times 10^1$
$-\Delta H_5$ (kJ mol^{-1})						$(2.71 \pm 0.07) \times 10^1$
E_{3a} (kJ mol^{-1}) [a]	$(5.19 \pm 0.09) \times 10^1$	$(5.34 \pm 0.08) \times 10^1$	$(5.30 \pm 0.10) \times 10^1$	$(5.82 \pm 0.08) \times 10^1$	$(5.93 \pm 0.07) \times 10^1$	$(7.37 \pm 0.07) \times 10^1$
E_{3b} (kJ mol^{-1})	$(6.49 \pm 0.09) \times 10^1$	$(5.41 \pm 0.08) \times 10^1$	$(4.90 \pm 0.10) \times 10^1$	$(5.49 \pm 0.08) \times 10^1$	$(5.56 \pm 0.07) \times 10^1$	$(7.35 \pm 0.07) \times 10^1$
E_{4a} (kJ mol^{-1})		$(1.24 \pm 0.08) \times 10^1$			$(9.05 \pm 0.08) \times 10^1$	$(1.18 \pm 0.01) \times 10^2$
E_{4b} (kJ mol^{-1})		$(8.64 \pm 0.08) \times 10^1$			$(2.42 \pm 0.01) \times 10^2$	$(2.48 \pm 0.07) \times 10^2$

[a] Parameter chosen by GSA. Value re-estimated using experimental data from the central point.

Table 6. Estimated Values of RSS and AIC for the Six Kinetic Models at Experimental Conditions for Prediction Capability Comparison

experimental run	M1	M2	M3	M4	M5	M6
		RSS $\times 10^5$ [mol^2 L^{-2}]				
6	3.07	0.76	0.35	0.44	0.29	0.41
7	10.5	9.49	0.36	0.32	0.29	0.60
8	1.94	2.57	0.50	0.96	0.97	0.78
9	1.86	1.67	0.57	0.52	0.43	0.37
AIC	−2093	−2129	−2653	−2588	−2611	−2585

estimates of K_0, which are about 100 to 10 times smaller than the referenced experimental value. The use of a toluene−avermectins solution instead of pure benzene could be adduced as being a possible cause affecting the dissociation equilibrium, but this question is left open. GSA clearly reveals that the involved linearly independent parameters (K_5, $-\Delta H_5$) are no-sensitive, and the gain of including this peripheral pathway is not significant. The number of adjustable parameters increases from 8 (model M3) to 18 (model M6) with 2 additional parameters linearly dependent (K_6, $-\Delta H_6$), as follows from eq 7.

Thus, GSA quantitative results strongly support that a reaction mechanism involving partial dissociation of RhCl(Ph$_3$P)$_3$ and catalytic cycle via the "hydride route" is fair enough for describing the hydrogenation of **Av** to **Iv** with Wilkinson's catalyst. Accordingly, we recognize the model M3 as the simplest plausible kinetic model which is able to describe the hydrogenation process with a data fitting capacity like that of more complex models. The model M3 has a relative lower complexity (only 8 parameters) and requires less computational effort because iterative algorithms are not necessary for solving model equations (there is an explicit expression for [RhCl(Ph$_3$P)$_2$S]). In fact, substitution of the positive quadratic root of eq 9 into

eqs 1−3 yields uncoupled first-order ODEs describing the hydrogenation rates. Moreover, for the isothermal hydrogenation process, ODEs straightforwardly yield exact solutions for **Av** and **Iv** concentrations in time domain. Furthermore, within the experimental range, it has been found that

$$K_0 \ll \frac{4[\text{Rh}]_0}{1 + K_1[\text{H}_2]} \tag{22}$$

and, consequently, the uncoupled first-order ODEs reduce to

$$\frac{d[\text{Av}_i]}{dt} = -k_{3i}K_1\sqrt{\frac{K_0[\text{Rh}]_0}{(1 + K_1[\text{H}_2])}}[\text{H}_2][\text{Av}_i], \quad i = a, b \tag{23}$$

which for isothermal hydrogenation process has the following analytical solution

$$[\text{Av}_i] = [\text{Av}_i]_0 \exp\left(-k_{3i}K_1\sqrt{\frac{[\text{Rh}]_0}{(1 + K_1[\text{H}_2])}}[\text{H}_2]t\right),$$
$$i = a, b \tag{24}$$

Equation 23 offers a straight way of describing the effects of the catalyst loading, avermectin concentration and hydrogen concentration on the hydrogenation rate. In fact, it is noticeable that (a) the hydrogenation rate is half-order with respect to the initial catalyst loading due to a partial dissociation of RhCl-(PPh$_3$)$_3$, as we remarked in a previous contribution.[7] This explanation seems to be more consistent than those based on the occurrence of catalyst dimerization[28] or a change from one active catalytic species to another less active at high catalyst loading.[47,48] (b) The reaction rate is first-order with respect to the concentration of these macrocyclic lactones, as also observed in hydrogenation of smaller olefins with Wilkinson's catalyst.[49] (c) The hydrogenation rate is lower than pseudo-first-order with
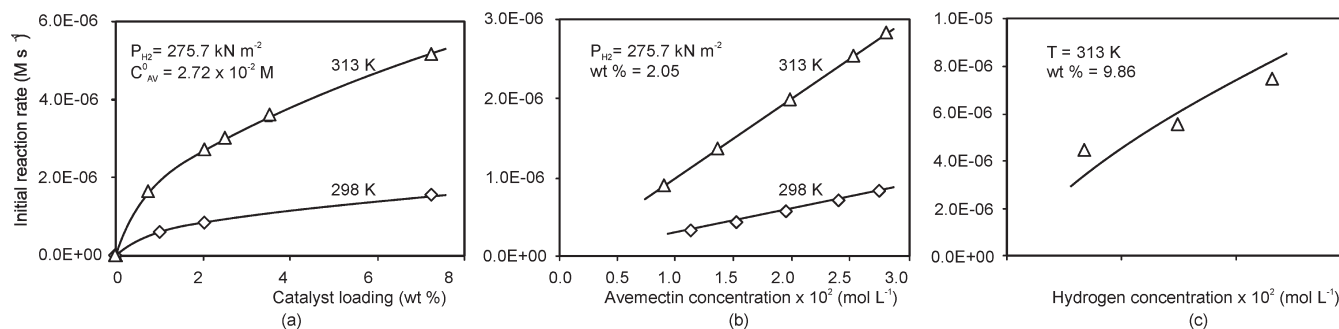
Figure 2. Dependence of the avermectin hydrogenation rate on (a) the catalyst loading, (b) avermectin concentration, and (c) hydrogen pressure. Full lines illustrate predictions of model M3.
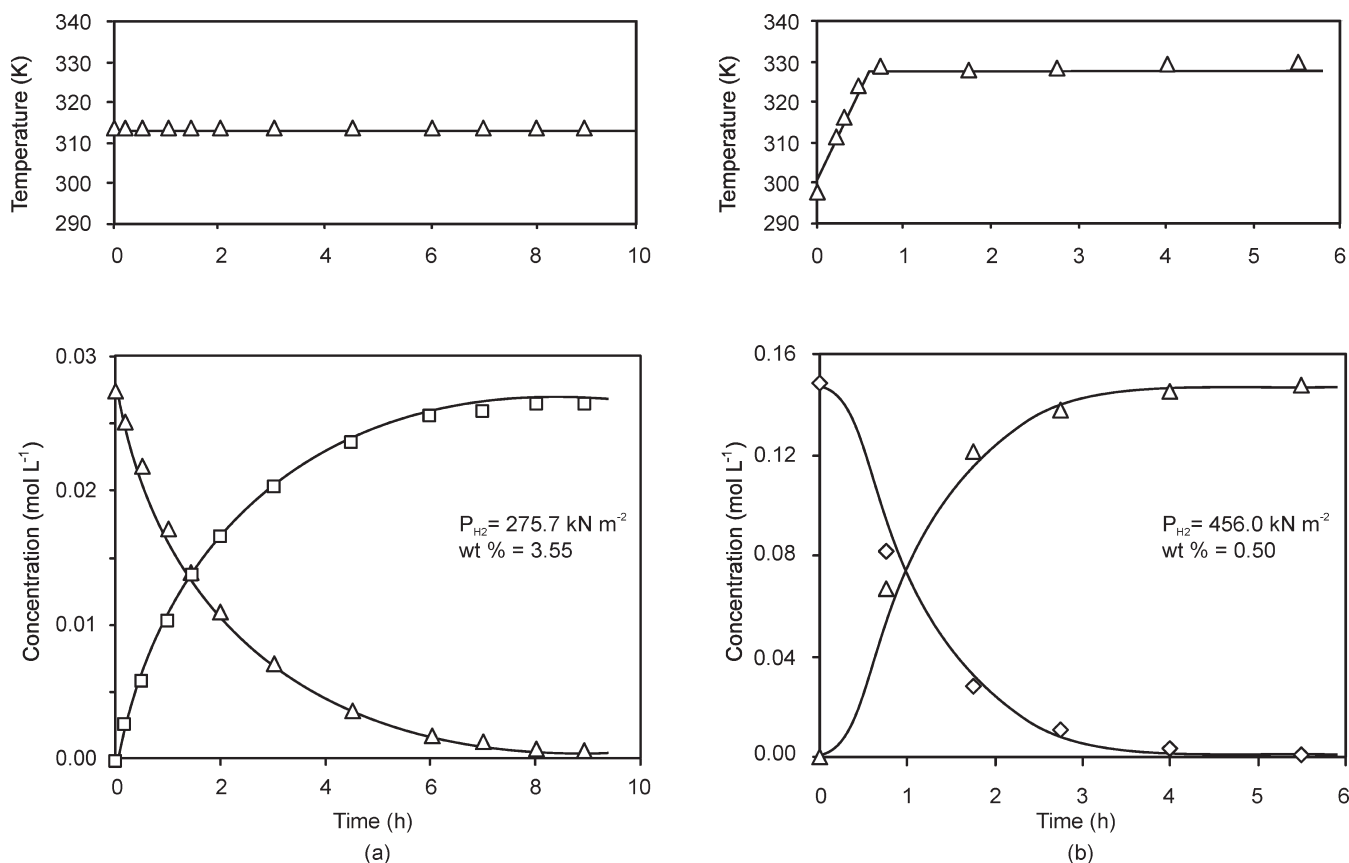

Figure 3. Experimental and predicted profiles during the hydrogenation of avermectin in (a) laboratory-scale reactor operating under isothermal conditions at hydrogen pressure of 275.7 kNm^{-2}; (b) industrial-scale reactor operating under nonisothermal conditions, at hydrogen pressure of 456.0 kNm^{-2}. Full lines illustrate predictions of model M3.

respect to the hydrogen concentration, as also remarked in a previous contribution.[7] Figure 2 shows that measured initial hydrogenation rates at different catalyst loading and avermectin concentrations are well predicted by model M3, but predictions in the hydrogen concentration domain are less accurate because the kinetic modeling was performed under isobaric conditions.

Since good fit does not necessarily imply good predictive capability, as an additional test for model performance evaluation, the prediction capability of model M3 was examined for both a laboratory-scale reactor operating under isothermal conditions and an industrial-scale reactor operating under nonisothermal mode until reaching the settled reaction temperature. Figure 3a exhibits the good-to-excellent capability of eq 24 to describe the experimental

Av and Iv concentration profiles from the isothermal laboratory-scale reactor. Figure 3b displays as predictions of model M3 fit to the experimental data quite well in the nonisothermal industrial-scale reactor. In the latter case, numerical integration of eq 23 was performed coupled to a temperature–time function describing the temperature profile in time domain. Although model prediction capability is not too good at the beginning stages of the process, the maximum differences between predicted and experimental data were found to be less than 8% which is slight, keeping in mind that both avermectin initial concentration and reaction pressure are quite far from those used to parametric estimations.

Finally, the traditional approach for parameters estimation has been implemented for allowing algorithm comparisons. RSS^k

Table 7. Estimated Values of RSS and AIC for the Six Kinetic Models at Experimental Conditions for Parameters Estimation

experimental run	RSS × 10⁴ with GSA						RSS × 10⁴ without GSA					
	M1	M2	M3	M4	M5	M6	M1	M2	M3	M4	M5	M6
1	3.37	2.26	0.08	0.15	0.12	0.15	3.14	2.88	1.29	0.19	0.18	0.19
2	4.70	5.37	0.89	0.50	0.57	0.47	5.71	5.55	0.02	0.49	0.43	0.41
3	6.51	7.63	0.11	0.05	0.14	0.04	3.06	2.95	3.13	1.44	0.05	0.05
4	1.25	0.68	0.13	0.27	0.29	0.26	4.05	3.87	1.66	0.66	1.00	0.58
AIC	−883	−874	−1247	−1270	−1242	−1265	−882	−880	−1020	−1122	−1187	−1224

and AIC^k values are shown in Table 7. Although AIC values for all six models are lowest when proposed algorithm is implemented, what deserves to be highlighted is the fact that GSA inclusion produces more information in regard to main reaction steps and more probable mechanisms that happen during avermectin hydrogenation reaction.

5. CONCLUSIONS

A rigorous modeling of avermectin hydrogenation with Wilkinson's catalyst could be very demanding and lead to overly complex models. Six mechanistic kinetic models of increasing complexity were scrutinized. GSA has been successfully applied to find the simplest model able to describe the hydrogenation process with a good data fitting capability. The calculated Sobol's first-order and total sensitivity indexes revealed that only very few and highly interacting parameters significantly influence the variance of the objective function, regardless which model is considered. Interestingly, the clear pattern of parameter relevance identified by GSA is consistent with the main reaction pathways involved in short-olefin hydrogenation, which are supported by careful kinetic and spectroscopic studies. Indeed, the most influencing parameters were found to be those related to the reaction pathway involving partial dissociation of the catalyst precursor $RhCl(PPh_3)_3$ and catalytic cycle through the "hydride route". More complex models were found to be over-parameterized because further reaction pathways only introduce additional uncertainty sources that individually have little influence on the variance of model predictions but the effects are spread over a major number of parameters.

Model $M3$ proved to be the simplest one for describing hydrogenation of avermectin B_1 (series a and b) to ivermectin in toluene solution with Wilkinson's catalyst within the operating condition range of industrial processes. The good performance of this model has been corroborated by comparing model predictions with experimental data from a laboratory-scale reactor and an industrial-scale reactor operating under isothermal and nonisothermal conditions, respectively. The model is simple to use while resulting in a significant computational effort saving because there is no need to perform iterative algorithms for solving model equations (algebraic and ODEs). An even, or still more, interesting feature is that $M3$ ODEs have an analytical solution for isothermal hydrogenation process. These peculiarities make model $M3$ easier for users to include into computational frameworks for design of the hydrogenation process and control systems of the most usual catalytic method for producing ivermectin.

■ APPENDIX

Imbalanced influence between pre-exponential (θ_1) and exponential (θ_2) constants has been taken into account in establishing the lower and upper boundary values of each temperature dependent parameter. We have equally distributed the total error between both uncertainty sources as follows.

The common functional description for both equilibrium and kinetic parameters variation with temperature can be written as

$$K = \theta_1 \exp\left(\frac{-\theta_2}{RT'}\right) \tag{A.1}$$

The total relative error (E_t) in parameter K value can be expressed as

$$\frac{dK}{K} = E_t \tag{A.2}$$

Taking into account eq A.1, the linearization by approximation of first-order Taylor-series expansion for function of two variables is

$$(dK)^2 = \sum_{i=1}^{2}\left(\frac{\partial K}{\partial \theta_i}\right)^2 d\theta_i^2 + 2\left|\prod_{i=1}^{2}\frac{\partial K}{\partial \theta_i}\right| COV_{\theta_1\theta_2} \tag{A.3}$$

Bearing in mind parameters estimation strategy, it is easily noticed that $COV_{\theta_1\theta_1}$ is null because experimental data for estimating θ_1 and θ_2 are independent sets.

Solving derivatives and after some algebra, we obtain

$$(dK)^2 = \left[\exp-\left(\frac{\theta_2}{RT'}\right)\right]^2 d\theta_1^2 + \left[\theta_1\left(\frac{1}{RT'}\right)\right.$$
$$\left.\exp-\left(\frac{\theta_2}{RT'}\right)\right]^2 d\theta_2^2 \tag{A.4}$$

$$\left(\frac{dK}{K}\right)^2 = \left(\frac{d\theta_1}{\theta_1}\right)^2 + \left(\frac{d\theta_2}{RT'}\right)^2 \tag{A.5}$$

In the attempt of having the same weight to each parameter, we define

$$\left(\frac{d\theta_1}{\theta_1}\right)^2 = \frac{E_t^2}{2} \rightarrow d\theta_1 = \frac{E_t\theta_1}{\sqrt{2}}$$
$$\left(\frac{d\theta_2}{RT'}\right)^2 = \frac{E_t^2}{2} \rightarrow d\theta_2 = \frac{E_t RT'}{\sqrt{2}} \tag{A.6}$$

where E_t is the total admitted error.

Finally, once E_i has been defined, parameter uncertainties for rough estimation can be directly computed.

■ AUTHOR INFORMATION

Corresponding Author
*E-mail: cqfina@santafe-conicet.gov.ar.

■ ACKNOWLEDGMENT

■ NOMENCLATURE

AIC = Akaike Information Criterion

AIC^k = value of AIC for kth model

$\mathbf{Av}_i$ = avermectin B$_i$ (i = a, b)

CCD = central composite design

E_i = activation energy for ith reaction

f = functional form of the model

GSA = global sensitivity analysis

$\mathbf{Iv}_i$ = ivermectin B$_i$ (i = a, b)

k = denotes kth kinetic model

k_{ij} = kinetic constant for ith reaction step and jth species

K_{ij} = equilibrium constant for i-th reaction step and jth species

$k_b a_b$ = gas−liquid overall mass-transfer coefficient

M_i = ith Model (i = 1, ..., 6)

N = number of experimental points used for parameters estimation

p = number of parameters being estimated

R = ideal gas constant

RDS = rate-determining step

RSS^k = residual sum of squares for kth model

r_H^{exp} = hydrogen consumption rate

S_i = first order sensitivity index with respect to ith parameter

ST_i = total effects sensitivity index with respect to ith parameter

SA = Sensitivity Analysis

t = time

T_r = reference temperature

T' = transformed temperature

$V(Y^k)$ = unconditional variance of Y^k

$V(\theta_i^k)$ = conditional variance of the parameter θ_i^k

$V(\theta_{-i}^k)$ = contribution to the variance of the Y^k output response attributable to the $p^k - 1$ remaining parameters

$\mathbf{w}^k$ = vector of known parameters representing operational conditions

$\mathbf{Y}^{exp}$ = matrix of experimental data to be fitted

$\mathbf{Y}^k(\boldsymbol{\theta}^k)$ = matrix of estimated data for kth model

$\mathbf{z}^k(t)$ = vector of concentrations of the active catalytic species included in the kth model

Special and Greek Symbols

[ ] = brackets denote concentration of the species

ΔH_i = entalpy change for ith reaction

θ^k = p-dimensional vector of kth model parameters with reliable set Θ^k

Γ = batch completion time

■ REFERENCES

(1) Fox, L. M. Ivermectin: Uses and Impact 20 Years On. *Curr. Opin. Infect. Dis.* **2006**, *19*, 588.

(2) Chabala, J. C.; Westfiel, N.; Fisher, M. H.; Bridgewater N. Selective Hydrogenation Products of C-076 Compounds and Derivatives Thereof. U.S. Patent 4,199,569; Merck & Co., 1980.

(3) Ma, X.-Y.; Wang, K.; Zhang, L.; Li, X.-J.; Li, R.-X. Selective Hydrogenation of Avermectin Catalyzed by Iridium−Phosphine Complexes. *Chin. J. Chem.* **2007**, *25*, 1503.

(4) Arlt, D.; Bonse, G.; Reisewitz, F. Process for The Preparation of Ivermectin U.S. Patent 5,656,748; Bayer Corp., 1997.

(5) Sogli, L.; Siviero; E.; Rossi, A.; Terrasan, D.; Bernasconi, E.; Terreros, P.; Salto, F. Process for the Preparation of Ivermectin. WO 9838201; Antobioticos Spa, 1998.

(6) Arlt, D.; Bonse, G. Method for the Preparation of Ivermectin. U. S. Patent 6,072,052; Bayer Corp., 2000.

(7) Zgolicz, P. D.; Cabrera, M. I.; Grau, R. J. A. Kinetics of the Homogeneous Hydrogenation of Avermectins Catalyzed by RhCl-(Ph$_3$P)$_3$ Complexes. *Appl. Catal. A.* **2005**, *283*, 99.

(8) Cabrera, M. I.; Zgolicz, P. D.; Grau, R.J.A. Kinetic Modeling of the Homogenoeus Hydrogenation of Avermectins Catalysed by In Situ formed RhCl(PPh$_3$P)$_3$ Complexes. *Appl. Catal. A* **2008**, *334*, 291.

(9) Chan, K.; Stefano, T.; Saltelli, A. Sensitivity Analysis of Model Output: Variance-Based Methods Make the Difference. *Proc. 1997 Winter Simulat. Conf.* **1997**, 261–268.

(10) Iman, R.; Helton, J. An Investigation of Uncertainty and Sensitivity Analysis Techniques for Computer Models. *Risk Anal.* **1988**, *8*, 71.

(11) Saltelli, A.; Tarantola, S.; Campolongo, F. Sensitivity Analysis as an Ingredient of Modeling. *Stat. Sci.* **2000**, *15*, 377.

(12) Saltelli, A.; Ratto, M.; Tarantola, S.; Campolongo, F. Sensitivity Analysis Practices. Strategies for Model-Based Inference. *Reliab. Eng. Syst. Safe.* **2006**, *91*, 1109.

(13) Sobol', I. M. Theorems and Examples on High Dimensional Model Representation. *Reliab. Eng. Syst. Safe.* **2003**, *79*, 187.

(14) Xu, C.; Gertner, G. Extending a Global Sensitivity Analysis Technique to Models with Correlated Parameters. *Comput. Stat. Data Anal.* **2007**, *51*, 5579.

(15) Marrel, A.; Iooss, B.; Laurent, B.; Roustant, O. Calculations of Sobol Indices for the Gaussian Process Metamodel. *Reliab. Eng. Syst. Safe.* **2009**, *94*, 742.

(16) Sobol', I. M.; Gatelli, T. D.; Kucherenko, S. S.; Mauntz, W. Estimating the Approximation Error when Fixing Unessential Factors in Global Sensitivity Analysis. *Reliab. Eng. Syst. Safe.* **2007**, *92*, 957.

(17) Saisana, A. S.; Tarantola, S. Uncertainty and Sensitivity Analysis Rechniques as Tools for the Quality Assessment of Composite Indicators. *J. R. Stat. Soc. A.* **2005**, *168*, 1.

(18) King, J. M. P.; Zhou, Y. Ranking Bioprocess Variables Using Global Sensitivity Analysis: A Case Study in Centrifugation. *Bioprocess Biosyst. Eng.* **2007**, *30*, 123.

(19) Saltelli, A.; Ratto, M. *Global Sensitivity Analysis. The Primer*: John Wiley & Sons Ltd., New York, 2008.

(20) Akaike, H. A new look at the statistical model identification. *IEEE Trans. Automat. Control* **1974**, *19* (6), 716.

(21) Sobol', I. M. Sensitivity Analysis for Non-linear Mathematical Models. *Math. Model. Comput. Exp.* **1993**, *1*, 407.

(22) Helton, J.; David, F. Latin Hypercube Sampling and the Propagation of Uncertainty in Analyses of Complex Systems. *Reliab. Eng. Syst. Safe.* **2003**, *81*, 23.

(23) Kucherenko, S.; Rodríguez-Fernández, M.; Pantelides, C.; Shah, N. Monte Carlo Evaluation of Derivative-Based Global Sensitivity Measures. *Reliab. Eng. Syst. Safe.* **2009**, *94*, 1135.

(24) Saltelli, A. Making Best Use of Model Valuations to Compute Sensitivity Indices. *Comput. Phys. Commun.* **2002**, *145*, 280.

(25) Marsaglia, G.; Zaman, A.; New, A Class of Random Number Generators. *Ann. Appl. Prob.* **1991**, *3*, 462.

(26) Bern, L.; Hell, M.; Schöön, N.-H. Kinetics of the Hydrogenation of Rapeseed Oil: II. Rate Equations of Chemical Reactions. *J. Am. Oil Chem. Soc.* **1975**, *52*, 182.

(27) Connolly, J. F. Thermodynamic Properties of Hydrogen in Benzene Solutions. *J. Chem. Phys.* **1962**, *36*, 2897.

(28) Osborn, J. A.; Jardine, F. H.; Young, J. F.; Wilkinson, G. The Preparation and Properties of Tri(triphenilphosphine)halogeno-Rhodium(I) and some Reactions Thereof Including Catalytic Homogeneous Hydrogenation of Olefins and Acetylenes and Their Derivatives. *J. Chem. Soc. (A).* **1966**, 1711.

(29) Jardine, F. H.; Osborn, J. A.; Wilkinson, G. Further Studies on the Homogeneous Hydrogenation of Olefins Using Tris(triphenylphosphine)halogenorhodium(I) Catalysts. *J. Chem. Soc. A.* **1967**, 1574.

(30) Montelatici, S.; van der Ent, A.; Osborn, J. A.; Wilkinson, G. Further Studies on the Homogeneous Hydrogenation of Olefins by use of Tris (tertiary phosphine)chlororhodium(I) Complexes. *J. Chem. Soc. A.* **1968**, 1054.

(31) Halpern, J. *Organotransition Metal Chemistry*; Ishii, Y., Tsutsui, M., Eds.; Plenum: New York, 1975; p 109.

(32) Halpern, J. Mechanistic Aspects of Homogeneous Catalysts. *Trans. Am. Crystallogr. Assoc.* **1978**, *14*, 59.

(33) Halpern, J. Mechanistic Aspects of Homogeneous Catalytic Hydrogenation and Related Processes. *Inorg. Chim. Acta* **1981**, *50*, 11.

(34) Halpern, J. Organometallic Chemistry at the Threshold of a New Millennium. Retrospect and Prospect. *Pure Appl. Chem.* **2001**, *73*, 209.

(35) Halpern, J.; Wong, C. S. Hydrogenation of Tris(triphenyl-phosphine) Chlororhodium(I). *J. Chem. Soc. Chem. Comm.* **1973**, *17*, 629.

(36) Halpern, J.; Okamoto, T.; Zakhariev, A. Mechanism of the Chlorotris(triphenylphosphine) Chlororhodium(I) —Catalysed Hydrogenation of Alkenes. The Reaction of Chlorodihydridotris(triphenyl-phosphine)rodhium(III) with Cyclohexene. *J. Mol. Catal.* **1977**, *2*, 65.

(37) Halpern, J.; Okamoto, T. Kinetic of the Migratory Insertion of Olefin into Rhodium-Hydrogen Bonds. Influence of Electronic Factors. *Inorg. Chim. Acta* **1984**, *89*, L53.

(38) Ohtani, Y.; Fujimoto, M.; Yamagishi, A. Kinetic Study on Dimerization of Chlorotris(tryphenilphosphine)rhodium(I) in Benzene. *Bull. Chem. Soc. Jpn.* **1976**, *49*, 1871.

(39) Ohtani, Y.; Fujimoto, M.; Yamagishi, A. Kinetic Study of Oxidative Addition and Replacement Reactions of Chlorotris(triphenyl-phosphine)rhodium(I) in Benzene. *Bull. Chem. Soc. Jpn.* **1977**, *50*, 1453.

(40) Ohtani, Y.; Fujimoto, M.; Yamagishi, A. The Rates of the Hydrogenation of the Coordinated Styrene and Acrylonitrile in a Rhodium—Olefin Complex $[RhClH_2(ol)(PPh_3)_2]$. *Bull. Chem. Soc. Jpn.* **1979**, *52*, 69.

(41) Rousseau, C.; Evrard, M.; Petit, F. Etude Cinetique de l'hydrogenation du Cyclohexene Catalysee par le Tris(triphenyl-phosphine)chlororhodium. *J. Mol. Catal.* **1978**, *3*, 309.

(42) Rousseau, C.; Evrard, M.; Petit, F. Etude Stereochimique de l'Hydrogenation en Phase Homogene d'Olefines Methyleniques Bicycliques Catalysee par un Tris(triphenylphosphine)halogeno-rhodium. *J. Mol. Catal.* **1979**, *5*, 163.

(43) Siegler, S.; Ohrt, D. The Kinetics and Mechanism of the Hydrogenation of Cyclohexene Catalyzed by Chlorotris (triphenylphosphine)rhodium(I) in Benzene. *Inorg. Nucl. Chem. Lett.* **1972**, *8*, 15.

(44) Meakin, P.; Jesson, J. P.; Tolman, C. A. The Nature of Chlorotris (triphenylphosphine)rhodium in Solution and Its Reaction with Hydrogen. *J. Am. Chem. Soc.* **1972**, *94*, 3240.

(45) Tolman, C. A.; Meakin, P. Z.; Lindner, D. L.; Jesson, J. P. Triarylphosphine, Hydride, and Ethylene Complexes of Rhodium(I) Choride. *J. Am. Chem. Soc.* **1974**, *96*, 2762.

(46) Arai, H.; Halpern, J. Dissociation of Tris(triphenylphospine)-chlororodium(I) in Solution. *J. Chem. Soc. D: Chem. Commm.* **1971**, *23*, 1571.

(47) O'Connor, C.; Wilkinson, G. Selective Homogeneous Hydrogenation of Alk-1-enes Using Hydrido-carbonyltris (triphenyl-phosphine) Rhodium(I) as Catalysts. *Inorg. Chem. Soc. (A).* **1968**, 2665.

(48) O'Connor, C.; Wilkinson, G. Non-selective in the Homogeneous Hydrogenation of Alkenes Using Chlorobis(Triarylphosphine) Rhodium(I) Catalysts. *Tetrahedron Lett.* **1969**, *18*, 1375.

(49) Mao, T.-F.; Rempel, G. L. Catalytic Hydrogenation of Nitile-Buatadiene Copolymers by Cationic Rhodium Complexes. *J. Mol. Catal. A. Chem.* **1998**, *135*, 121.

4263

dx.doi.org/10.1021/ie101289h |*Ind. Eng. Chem. Res.* 2011, 50, 4252–4263